TWO-WAVELENGTH LIDAR MEASUREMENT TECHNIQUE AND DATA ON STRATOSPHERIC AEROSOL OPTICAL PARAMETERS OF

A.P. Ivanov, A.P. Tchaikovsky, V.N. Shcherbakov, F.P. Osipenko, M.M. Korol, and S.B. Tauroginskaya

Belarussian Institute of Physics, Minsk
Received July 15, 1996

Since Mt. Pinatubo eruption, regular lidar sounding of the stratospheric aerosol layer has been carried out at the Institute of Physics, Belarus Academy of Sciences (Minsk, 53.85 °N, 27.5 °E) by means of a two-wavelength polarization lidar. The technique and results of the laser sounding of the stratospheric aerosol are presented in this paper.

1. INTRODUCTION

As a result of Mt. Pinatubo eruption in June, 1991, approximately 10 Mtn of sulfur dioxide were emitted into the atmosphere thus causing formation of dense aerosol clouds in the stratosphere. Regular lidar sounding of the stratospheric aerosol layer (SAL) has been carried out at the lidar station, of the Institute of Physics, Belarus Academy of Sciences (Minsk, 53.85 °N, 27.5 °E). The measurements have been performed using a two-wavelength lidar ANF-314 (see Ref. 1). Simultaneously the lidar measures depolarization of the aerosol backscatter.

The parameters measured with the lidar make a minimum set of data providing information about both spatiotemporal dynamics of the aerosol layer and changes in microstructure of aerosol particles during the formation and transformation of the SAL. In this paper, we describe some peculiarities in the measurement technique and data processing algorithms reflecting specific features of our two-wavelength polarization sounding. The experimental results presented here well demonstrate the capabilities of the facility and technique used.

2. TECHNIQUE FOR MEASURING THE SAL PARAMETERS BY MEANS OF A TWO-WAVELENGTH POLARIZATION LIDAR

The data of two-wavelength polarization sounding of the SAL, allowed us to reconstruct the following optical parameters:

− the backscattering ratio

$$R(h, \lambda_1) = [\beta_a(h, \lambda_1) + \beta_m(h, \lambda_1)] / \beta_m(h, \lambda_1),$$

where $\beta_a(h, \lambda_1)$ and $\beta_m(h, \lambda_1)$ are the aerosol and molecular backscattering coefficients at $\lambda_1 = 532$ nm;

− the ratio between the aerosol backscattering coefficients at two wavelengths

$$\gamma(h) = \beta_a(h, \lambda_2) / \beta_a(h, \lambda_1),$$

where $\lambda_2 = 1064$ nm;

− the degree of depolarization of the aerosol backscatter $Q_a(h)$.

A set of $R(h, \lambda_1)$ profiles bears information about the dynamics of vertical stratification and concentration of aerosol in the stratosphere. The measurement data on $\gamma(h)$ and $Q_a(h)$ allow us to detect changes in the microstructure of aerosol particles during the SAL transformation after the eruption.

When processing lidar return signals we used, conventional methods of determining the minimum in function $R(h, \lambda)$ (see Ref. 2). Peculiarity of two-wavelength sounding required an additional consideration of the question: an estimation of the information content of sounding and development of calculation procedures for the aerosol decay, and algorithms for simultaneously processing the data obtained. Analysis of experimental data and simulation of the SAL optical parameters transformation have been made on the basis of statistical processing using expansion of empirical functions over natural orthogonal components (see Ref. 3).

2.1. Relationship between parameter γ and size of aerosol particles

Changes in the spectral behavior of the backscattering coefficient in the SAL are primarily due to transformation of the size distribution of aerosol particles $n(r)$. When solving a lot of applied problems, single-modal distribution function $n(r)$ (see Refs. 4–6), in particular, lognormal one of the following form:

$$n(r) = \frac{1}{\sqrt{2\pi}\, r\, \ln\sigma} \exp\left\{ -\frac{\ln^2 r / r_0}{2\ln^2\sigma} \right\} \qquad (1)$$

are used in calculations of the optical parameters. If the size distribution is described by the function (1), measurements of γ allows parameter r_0 to be estimated. The uncertainty of this estimation due to possible changes in σ is shown in Fig. 1, where γ has been calculated based on the model of single-mode lognormal

distribution for two widths of the distribution function (σ = 1.604 and 1.92). The ranges of r_0 and σ changes correspond to values normally accepted for simulation of the distribution. Tendency to γ increase with r_0 is seen, but in the vicinity of r_0 = 0.1 this dependence is nonmonotonic. It is important since the value r_0 = 0.12 μm is typical for the model of the background stratospheric aerosol.
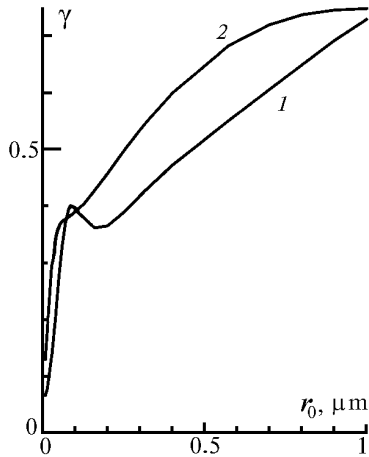
FIG. 1. *The ratio between the aerosol backscattering coefficients as a function of γ parameters r_0 and σ of the size distribution function. Curve 1 corresponds to σ = 1.604, curve 2 corresponds to σ = 1.92.*

In the case of different $n(r)$ the aerosol optical parameters will be similar if the efficient parameters of the distribution function, $r_{3/2}$ and σ_{eff} = = $(r_{4/3}/r_{3/2}) - 1$, are close to each other. In particular, it is true for the modified gamma-distribution (see Ref. 4) used for the aerosol simulation in Ref. 6.

Measurements of $n(r)$ (see Refs. 7−9) show that in some cases the stratospheric aerosol was in fact a mixture of several fractions. Along with a component similar to the background one, modes of "fine" and "large" particles are observed. Therefore, in the absence of additional information on $n(r)$, results of measurements of γ are only an indicator of changes in the particle size and only demonstrate the tendency in changes of their efficient radius.

2.2. Estimation of the extinction coefficient from the two-wavelength lidar data

During the period from Dec. 1991 to Jan. 1992 the aerosol optical thickness was close to 0.2 at the wavelength of 532 nm. This is an essential value, which must be correctly taken into account when processing lidar data. In the single-wavelength sensing the aerosol optical thickness is estimated assuming the aerosol backscattering phase function. In the case of two-wavelength sounding the relationship between the aerosol extinction and backscatter can be determined.

Because of variations in $n(r)$ this relationship is statistic in nature.

We have estimated the aerosol extinction coefficient $\varepsilon_a(\lambda_i)$ from the values of the aerosol backscatter using linear regression:

$$\varepsilon_a(\lambda_i) = \sum_{j=1}^{2} c_{ij} \, \beta_a(\lambda_j) \, , \qquad (2)$$

where coefficients c_{ij} are determined by the algorithm described in Ref. 10. In this case the range of $n(r)$ changes should be preset. Peculiarity of construction of the estimation (2) are shown in Fig. 2, where the ratio $\varepsilon_a(\lambda_1)/\beta_a(\lambda_1)$ at λ = 532 nm versus γ is presented for different stratospheric aerosol models taken from Ref. 4:

1) single-mode lognormal distribution $n(r)$, r_0 varies at a constant value σ = 1.604;

2) the aerosol is considered as a mixture of "fine" (r_0 = 0.04 μm, σ = 1.604) and background (r_0 = 0.12 μm, σ = 1.604) fractions at variable relative concentration;

2) the aerosol is considered as a mixture of "large" (r_0 = 0.572 μm, σ = 1.604) and background fractions at variable relative concentration.
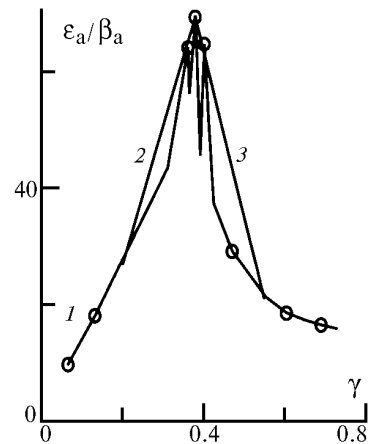
FIG. 2. *The ratio $\varepsilon_a(\lambda_1)/\beta_a(\lambda_1)$ at λ_1 = 532 nm versus parameter γ for the following models of the size distribution: single-mode lognormal distribution (curve 1), fine particles and background fraction (curve 2), large particles and background fraction (curve 3).*

Qualitatively similar dependences have been obtained for $\varepsilon_a(\lambda_2)/\beta_a(\lambda_2)$ (λ_2 = 1064 nm).

It is evident that the linear approximation for the extinction coefficient $\varepsilon_a(\lambda_i)$ estimate should be made separately for fine and large particles. We have constructed two estimations like (2) for both wavelengths and $\gamma \leq 0.38$ and $\gamma \geq 0.38$. Such a representation of $\varepsilon_a(\lambda_i)$ in terms of the backscattering coefficients at two wavelengths describes adequately the situation when the stratospheric aerosol can be considered as a combination of two fractions, namely,

"fine" and background or "large" and background fractions. In this case the error in estimate (2) at $\lambda_1 = 532$ nm is about 20%. However, the estimate is inconsistent with the model of "fine" and "large" fractions.

2.3. Algorithm for calculating the backscattering ratio profiles based on processing the data of two-wavelength sounding

The interrelation between the recorded profiles of the number of accumulated photons $N(x_i, z)$ and optical parameters of the atmosphere is described by a set of lidar equations of the following form:

$$N(\lambda_i, z) = A(\lambda_i, z) \, W_0(\lambda_i) \, z^{-2} \, \beta(\lambda_i, z) \times$$

$$\times \exp\left(-2 \int_0^z \varepsilon(\lambda_i, z') \, \mathrm{d}z'\right). \qquad (3)$$

Here z is the current coordinate along the sounding path, λ is the wavelength, $i = 1,\dots,n$, n is the number of wavelengths, $A(\lambda_i, z)$ is the lidar geometric function, $W_0(\lambda_i)$ is the energy of sounding pulse,

$$\beta(\lambda_i, z) = \beta_a(\lambda_i, z) + \beta_m(\lambda_i, z) , \qquad (4)$$

$$\varepsilon(\lambda_i, z) = \varepsilon_a(\lambda_i, z) + \varepsilon_m(\lambda_i, z) \qquad (5)$$

are the profiles of the backscattering and extinction coefficients, respectively, aerosol and molecular values are marked with the subscript a and m, respectively.

At large distance from the lidar system the function $A(\lambda_i, z)$ may be considered constant. By analogy with the conventional procedure for single-frequency sounding (see Ref. 2) one can choose some point z_0 at which values of the scattering ratio $R(\lambda_i, z_0) = [\beta_a(\lambda_i, z_0) + \beta_m(\lambda_i, z_0)] / \beta_m(\lambda_i, z_0)$ can be preset. This point generally corresponds to the minimum in $R(\lambda_i, z)$ and is chosen in the region where contribution from the aerosol scattering is taken to be minimum. In this case $R(\lambda_i, z_0) = R_{\min}(\lambda_i)$ is close to unit. From Eqs. 3–5 it follows that:

$$R(\lambda_i, z) = \frac{z^2 \, N(\lambda_i, z) \, L^2(\lambda_i, 0, z_0) \, \beta_m(\lambda_i, z_0)}{z_0^2 \, N(\lambda_i, z_0) \, L^2(\lambda_i, 0, z) \, \beta_m(z)} R_{\min}(\lambda_i) , \qquad (6)$$

where

$$L^2(\lambda_i, 0, z) = L_a^2(\lambda_i, 0, z) \, L_m^2(\lambda_i, 0, z) ,$$

$$L_a^2(\lambda_i, 0, z) = \exp\left[-2 \int_0^z \varepsilon_a(\lambda_i, z') \, \mathrm{d}z'\right],$$

$$L_m^2(\lambda_i, 0, z) = \exp\left[-2 \int_0^z \varepsilon_m(\lambda_i, z') \, \mathrm{d}z'\right].$$

The ratio $L_m^2(0, z_0) / L_m^2(0, z)$ is assumed to be known and calculated from the data of meteorological measurements. Equation (6) may be written in the following form:

$$R(\lambda_i, z) = R^*(\lambda_i, z) \exp\left[-2 \int_z^{z_0} \varepsilon_a(\lambda_i, z') \, \mathrm{d}z'\right], \qquad (7)$$

where

$$R^*(\lambda_i, z) = \frac{z^2 \, N(\lambda_i, z) \, L_m^2(\lambda_i, 0, z_0) \, \beta_m(\lambda_i, z_0)}{z_0^2 \, N(\lambda_i, z_0) \, L_m^2(\lambda_i, 0, z) \, \beta_m(z)} R_{\min}(\lambda_i). \qquad (8)$$

The function $R^*(\lambda_1, z)$ is found from experimentally measured values and by introducing a priori parameters of $R_{\min}(\lambda_i)$. The scattering ratio profile $R(\lambda_1, z)$ coincides with $R^*(\lambda_1, z)$ if $L_a^2(0, z_0) / L_a^2(0, z) = 1$, i.e. when the aerosol extinction in the interval $[z_0, z]$ is ignored. Equation (7) demonstrates how the aerosol extinction influences the results of calculations of the scattering ratio. Besides, Eqs. (7) is a set of equations for calculating profiles $R(\lambda_i, z)$.

Generally, the system of Eqs. (7) is a set of n equations and while having $2n$ unknowns. Let us complete determination of the set by introducing Eq. 2 and using the representation $\beta_a(\lambda_i, z) = (R(\lambda_i, z) - 1) \beta_m(\lambda_i, z)$. Then Eq. (7) can be written, with the account for Eqs. (2) and (8), as:

$$R(\lambda_i, z) =$$

$$= F(\lambda_i, z) \exp\left(-2 \sum_j C_{ij} \int_z^{z_0} R(\lambda_j, z') \, \beta_m(\lambda_i, z) \, \mathrm{d}z'\right), \qquad (9)$$

where

$$F(\lambda_i, z) = R^*(\lambda_i, z) \exp\left(2 \sum_j C_{ij} \int_z^{z_0} \beta_m(\lambda_j, z') \, \mathrm{d}z'\right) \qquad (10)$$

are known functions. As a result, we obtain a complete set of equations (9) for reconstructing the profiles $R(\lambda_i, z)$.

Let us consider the case when the sounding path is timegated in regular intervals Δz. Then, instead of Eq. (10) we experimentally obtain a matrix F_{ik}, where i is a number of wavelength, k is a number of a time gate. Using the approximation of integrals by the

formula of trapezoid one can rewrite Eq. (9) in the following form (the case of $z_k > z_0$, z_0 is the reference point):

$$R_{ik} = F_{ik} \exp\left\{ \Delta z \left(\sum_j C_{ij} R_{j0} + \sum_{\nu=1}^{k-1} \sum_j 2\, C_{ij} R_{j\nu} + \sum_j C_{ij} R_{jk} \right) \right\},$$
(11)

where $R_{ik} = R(\lambda_i, z_k)$; $F_{ik} = F(\lambda_i, z_k)$. For $z_k < z_0$ corresponding formula is similar to Eq. (11) except for minus sign of Δz in the exponent. Equation (11) can be solved by the iteration method (see, for example, Ref. 11).

2.4. Measurement of depolarization of the aerosol backscatter

The measurements of the backscattering depolarization in the case of sounding with linearly polarized radiation have been carried out to detect layers with nonspherical particles of volcanic ashes, overcooling of the stratosphere or crystal cloud formation. If the concentration of aerosol component is low, depolarization of the lidar return due to molecular scattering strongly masks the effect and makes the identification of nonspherical aerosol particles in the stratosphere too difficult. Therefore, the measurement technique includes special lidar calibration which provides high precision of measurements of local signal depolarization and eliminates, when processing data, the contribution of molecular scattering. Degree of depolarization of the inverse scattering signal may be calculated according to the following expression (see Ref. 12):

$$Q_a(h) = [R_1(h)\, Q(h) - \omega] / [R_1(h) - 1] ,$$
(12)

where ω is the degree of depolarization due to molecular scattering, $R_1(h)$ is calculated similarly to $R(h)$ for the component of the backscatter whose polarization is identical to that of the sounding pulse, $Q(h)$ is the degree of depolarization of return signal. For $Q(h)$ to be measured with low error (of the order of 2%), we have carried out additional sounding sessions using sounding radiation with the polarization plane oriented at 45° angle with respect to the polarization plane of analyzers in the lidar optical receiver.

3. EXPERIMENTAL RESULTS

The early though weak manifestations of Mt. Pinatubo eruption were detected at the lidar station (Minsk) on June 11, 1991. Maximum of the ratio $R(h, \lambda_1)$ was recorded at a height of 15.5 km. The maximum values of the parameter R, integral aerosol backscattering coefficients, and optical thickness of the atmosphere were observed during Dec. 1991–Feb. 1992. As the optical thickness of the SAL increases, changes in $R(h, \lambda_1)$ occur similarly to

corresponding data obtained at the lidar station in Garmishpartenkirhen (see Refs. 13, 14) with a time delay of several days.

As our measurements demonstrated, transformation of the profile $\gamma(h)$ from an irregular, at the early stage, to a relatively stable one throughout the first year after the eruption. Typically, $\gamma(h)$ decreased with height during this time.
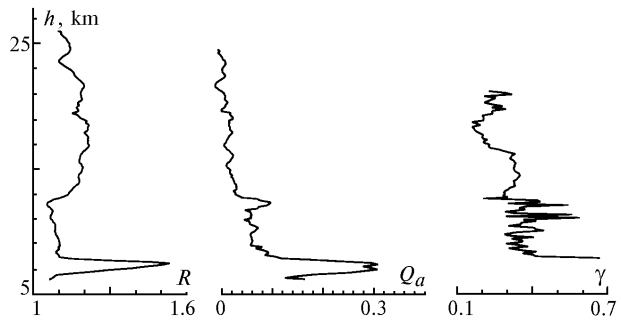
FIG. 3. Profiles of the parameters $R(h, \lambda_1)$, (γ) and $Q_a(h)$ according to the sounding data (Sept. 16, 1994).

Measurements of the depolarization $Q_a(h)$ showed that in some cases layers of nonspherical particles formed in the lower part of the SAL. In particular, such a layer was detected during measurements under the LITE program in Sep. 1994. Figure 3 demonstrates the data obtained on Sept. 16, 1994. Increase in depolarization along with the appearance of local maxima in $\gamma(h)$ has been revealed in the lower stratosphere. All these facts are indicative of the existence of a reasonably large nonspherical particles at heights 9 to 14 km. The height of the tropopause was 8 km. The results of measurements of $R(h, \lambda_1)$ performed during that period were related to the data obtained over Belarus with a spaceborne lidar. The latter were put at our disposal by Dr. Mary Osborn. The variance of $R(h, \lambda_1)$ comprised 3 to 5%.

4. DATA PROCESSING TECHNIQUE

From the data of lidar sounding of the SAL, we have obtained sets of experimental data on changes in $R(h, \lambda_1)$, $\gamma(h)$ and $Q_a(h)$ after Mt.Pinatubo eruption. The goal of the following processing of these sets was to decrease the bulk of numerical data with minimum information losses and to find substantial components in $R(h, \lambda_1)$ changes. Therewith construction of relatively simple models, describing temporal transformation of the SAL and comparison of the experimental results obtained at different lidar stations became possible.

In this paper, the technique of statistical analysis is demonstrated using the processing of the sets of parameters $R(h)$ as an example. Expansion of vectors $R(h_i)$, $i = 1, \ldots, N$ (N is a number of levels) over characteristic vectors of the covariance matrix was made. As our calculations showed, such a representation is more efficient when

logarithms of the vectors $\ln[R(h_i)]$ are considered instead of the vectors themselves. The profiles of average value of $\langle \ln[R_n(h_i)]\rangle$, correlation matrix $W_{ij} = \langle \ln[R_n(h_i)]\ln[R_m(h_j)]\rangle$, eigenvectors $\xi_k(h_i)$, and eigenvalues δ_k of $W_{i,j}$ (here n is the profile number) were calculated. The sum of the first three eigenvalues δ_k of $W_{i,j}$ was found to be equal to 0.91 of their total sum. Therefore, the following expression describes 91% of the changes in $\ln[R_n(h_i)]$:

$$\ln[R_n(h_i)] \cong \langle \ln[R_n(h_i)]\rangle + \sum_{k=1}^{3} q_{n,k}\, \xi_k(h_i) \; . \qquad (13)$$

In our case, three coefficients $q_{n,k}$ bear the main information about the profile $\ln[R_n(h_i)]$. Thus, the set of data on $\ln[R_n(h_i)]$ was converted into the set of coefficients $q_{n,k}$. The latter, in its turn, was divided into six groups by the algorithm of objective classification ISODATA (see Ref. 15). Thereby, classification of $\ln[R_n(h_i)]$ was achieved. The distance between the points in the three-dimensional space of coefficients $q_{n,k}$ corresponding to the profiles under

classification was used as a criterion for distinguishing between the profiles.

Figure 4 depicts a profile $\langle \ln[R_n(h_i)]\rangle$ and the average profiles $\langle \ln[R(h_i)]\rangle_p$ calculated from Eq. (3) for each of the six classes ($p = 1...6$). The profiles from different classes differ in their heights and maximum values.
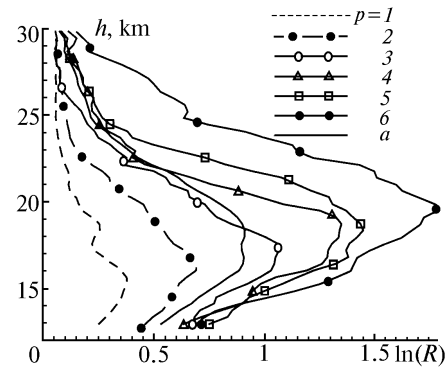
FIG. 4. Average profiles $\langle \ln[R(h_i)]\rangle_p$ for each class ($p = 1...6$) and the average profile $\langle \ln[R_n(h_i)]\rangle$.
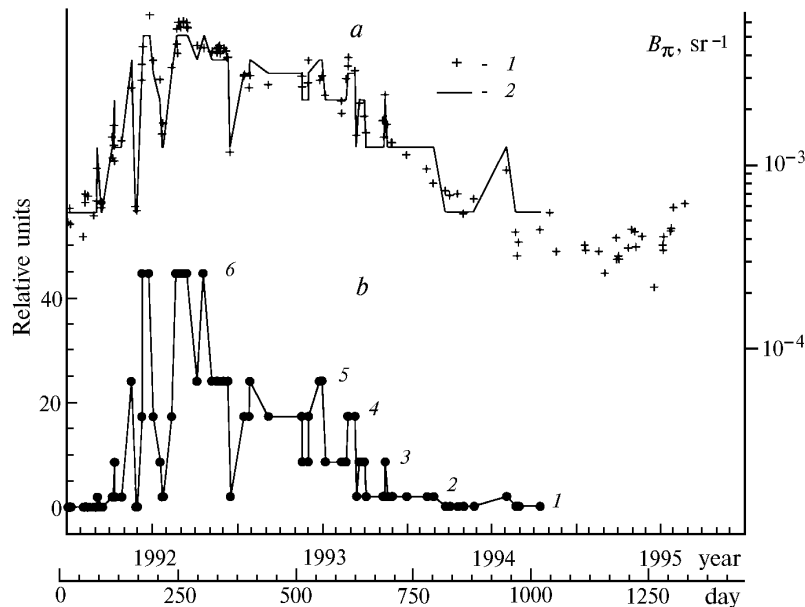
FIG. 5. Temporal behavior of the optical parameters of SAL. Curve 1 and 2 correspond to measured and reconstructed, from statistical model, values of the integral backscattering coefficient B_π, respectively (a). Process of transformation of the profiles $\ln[R(h_i)]$ over classes $p = 1...6$ after the eruption (b).

Figure 5,b demonstrates the change of $\ln[R(h_i)]$ classes due to transformations in SAL. Numbers of classes are shown by figures at the corresponding points ($p = 1 ... 6$). The distance, in space of the coefficients $q_{n,k}$, between the centers of the first and other classes to which every point relates is plotted on the ordinate (left scale).

The statistical analysis performed allowed us to present the information on changes in the height structure of the SAL, $R(h)$, in an extremely compact form of a

small amount of average profiles $R(h_i)$ of different classes (see Fig. 4) which transition from one class to another occur according to Fig. 5,b. These results can be considered as "statistical" model characterizing the transformation of the SAL optical parameters in our region. In particular, an increase in maximum of the layer and buildup of aerosol concentration during the aerosol layer formation and inverse processes during the SAL relaxation to the background state are described. Calculated from this model values of the integral

backscattering coefficient B_π in the layer at heights 13–30 km are plotted by solid line in Fig. 5,*a*. The rms deviation from directly measured values comprises only 16%.

REFERENCES

1. A.I. Borodavko, N.P. Vorobei, V.I. Gubskii, et. al., Atm. Opt. **1**, No. 3, 109–115 (1988).

2. P.B. Russel, J.T. Swissler, and P.M. McCormick, Appl. Opt. **18**, No.22, 3783–3797 (1979).

3. A.M. Obukhov, Izv. Akad. Nauk SSSR, Geofiz. No. 3, 552–554 (1960).

4. J. Lenoble and C. Brogniez, Appl. Opt. **24**, No. 7, 1054–1063 (1985).

5. P.B. Russel, J.T. Swissler, M.P. McCormick, W.P. Chu, J.M. Livingston, and T.J. Pepin, J. of the Atmosph. Sciences **38**, No. 6, 1279–1294 (1981).

6. *A preliminary cloudless standard atmosphere for radiation computation. International Association for Meteorology and Atmospheric Physics. Radiation Commission.* Boulder, Colorado. USA. 1984. 53 pp.

7. T.Deshier, D.J. Hofmann, B.J. Johnson, and W.R. Rozier, Geophys. Research Lett. **19**, No. 2, 199–202 (1992).

8. J. Goodman, *ibid*. **21**, No. 12, 2179–2182 (1994).

9. L.W. Thomason, *ibid*. **19**, No. 21, 2179–2182 (1992).

10. S.B. Tauroginskaya, A.P. Tchaikovsky and V.N. Shcherbakov, Atmos. Oceanic Opt. **7**, No. 10, 758–760 (1994).

11. I.E. Naats, *Theory of Multifrequency Laser Sounding of the Atmosphere* (Nauka, Novosibirsk, 1980), 158 pp.

12. A.P. Tchaikovsky, Atm. Opt. **3**, No. 11, 1107–1109 (1990).

13. H. Jager, V. Freudenthaler and F. Homburg, *Abstracts of Papers of the 17-th International Laser Radar Conference*, Sendai, Japan, 1994, pp.371–374.

14. H. Jager, Geophys. Research. Lett. **19**, No. 2, 191–194 (1994).

15. D.T. Too and R.K. Gonsales, *The principles of recognition of images* (Mir, Moscow, 1978), 441 pp.